Finite Element Analysis for Engine Cylinder head in Ansys

Dr.B.Sudarshan[1], Associate professor, Center for Research and Innovation (CRI) & K.S.R.M.College of Engineering, Kadapa, Andhra Pradesh, India. Email: sudarshan765@gmail.com
Mr.Subhajith Roy[2], Student, Department of Mechanical engineering, K.S.R.M.College of Engineering, Kadapa, Andhra Pradesh, India. Email: roysubhajith@gmail.com

ABSTRACT:

The application of thermal analysis concept is leading towards engineering design during engine development in the thermal equilibrium condition. The life and output potential of such engines is strongly connected to the working temperature of specified components. Thus, accurate temperature predictions are an essential pre-requisite to the continuing engine evolution. From a material science prospect, temperature field in an engine, important elements like cylinder head and block is needed to judge element practicality below specific load and conditions. In order to focus on this issue, on wide-ranging experimental and analytical study to investigate temperature fields in four-cylinder head and block of recently developed diesel engines. A comprehensive thermal analysis was carried out on the engine in the various conditions with the help of Ansys software. The effect of heat transfer differences at various loads of an engine.

Keywords: Heat transfer, Experimental thermal analysis, Ansys.

1. INTRODUCTION

The peak temperatures of burning gases within the cylinder of diesel engines are of the order of 2700k. to stop heating, the most temperatures of the metal surfaces intromission the combustion chamber are restricted an excessive amount of lower values and, therefore, cooling should be provided for the cylinder, plate, and piston. The substantial heat fluxes and temperature, no uniformities arising from these conditions cause thermal stresses, that additional increase the otherwise important mechanical loading from combustion pressures. the look should take under consideration of these concerns to confirm a straightforward operation of engines, which, particularly within the case of elements of advanced style, needs an extended analysis supported careful data of all the processes concerned.

The plate is one among the foremost sophisticated elements of an interior combustion engine. it's directly exposed to high combustion pressures and temperatures. additionally, it has to house intake and valve ports, the fuel, and complicated cooling passages. Compliance with of these necessities ends up in several compromises in style. As a result, cylinder heads tend to fail to operate (distortions, fatigue cracking) because of heating in regions of restricted cooling. However, thermal and mechanical stresses in various plate and block are going to be on top of the naturally aspirated engine and it should force coming up with some elements or dynamical the fabric. therefore the specialize in work temperature fields in plate and block of a recently developed engine.

during this case, the stress on the problematic regions around the valve seats and slender bridges between valves. These regions expertise particularly severe thermal loading, as they receive heat not solely from in-cylinder burning gases throughout the combustion amount however additionally from burned gases flowing through the valve and on the exhaust-port walls during the exhaust. though the temperatures of exhaust gases are considerably not up to peak in-cylinder temperatures, fast movement of flowing gases there promotes the warmth transfer to the walls. Most of the warmth accumulated within the valve is rejected through the contact surface of the valve seat. Therefore, any deformations of those elements amid improper contact and also the incidence of discharge on the conic valve contact face dramatically increase

the thermal loading of the valves and, therefore, might cause their destruction. A detailed finite element heat-transfer analysis will offer valuable info on the temperature distribution within the overall assembly of the plate, particularly in those regions wherever experimental data is sort of not possible to collect. Moreover, this is often the primary logical stage of plate strength analysis.

In the next step, the temperature and mechanical stresses should be analyzed exploitation temperature field and pressure (and alternative mechanical hundreds, e.g., belt pre-stress). The ensuing displacement/stress fields are also used for the analysis of operational conditions, e.g., the contact pressure between valves and valve port uniformity, also as strength and failure resistance of the assembly. Such info contributes to an in-depth below standing of the thermal and mechanical processes within the cylinder-head assembly under engine operation, that may be a requirement for more improvement of engine style.

1.1 Engine heat transfer

The importance of engine heat transfer is obvious because of its role in engine potency, emission, endurance, friction, and lubrication. in an exceedingly typical IC engine, the supply of heat generation is burning of air-fuel mixture within the cylinder(s). In these engines but 1/2, the generated heat within the operating fluid produces power and another half is dissipated from other ways in the engine via 3 modes: physical phenomenon, convection, and radiation. It is, therefore, a posh method that depends upon varied parameters like properties of operating fluid and combustion parameters, engine pure mathematics and material specifications, cooling and lubrication system style and characteristics of utilized fluids within them. The quality would be larger once considering that heat transfer takes place below conditions of variable pressure level, temperature and also the extent of the combustion chamber through the cycle.

Engines have evolved apace within the last decade mostly as a result of emissions legislation, however, heat transfer modeling techniques haven't unbroken pace with these developments. The ordinarily used models to predict the warmth flux arising from combustion gases, specifically those of Annand [1], and Woschni [2], are supported noncurrent engine technology. At the time once these strategies were projected, most of the fashionable options already mentioned within the case of latest engines failed to exist or weren't widely used. These models predict the heat transfer constant superb round the combustion stroke. However, at the opposite crank angles specifically within the growth stroke, they need a deviation from the particular knowledge [3]. What is more, the Woschni and Annand models don't seem to be ready to predict the native convective heat transfer in an exceedingly spark ignition engine okay [4, 5] These facts recommend a necessity for updated predictions of thermal conditions, particularly, in-cylinder temperatures and temperature profiles within the block and plate [6,7]. The potential edges procurable from higher thermal predictions embrace increased cooling systems (smaller and lighter pumps and warmth exchangers) [8–11], reduced thermal distortion (lower friction and optimized seal assembly), and better power [12]. Improved predictions of engine temperatures are vital for applying procedure strategies (CFD and FEA) [9–11]. The accuracy of laptop programs depends, together with the provision of laptop power, on the specification of boundary conditions.

Therefore, the applying of those promising techniques can get pleasure from enhancements within the strategies to predict thermal boundary conditions. Ultimately, these edges are probably to contribute to decreased fuel consumption and lower emissions in automobiles.

2. CYLINDER-BLOCK ASSEMBLY

In the present study, the plate of an enormous turbocharged direct-injection (DI) diesel is analyzed. The engine is employed in power generation units. the fundamental parameters of the engine are: bore 275 mm, stroke 330 mm, most brake mean effective pressure 1.95 MPa, nominal speed 760 rpm.

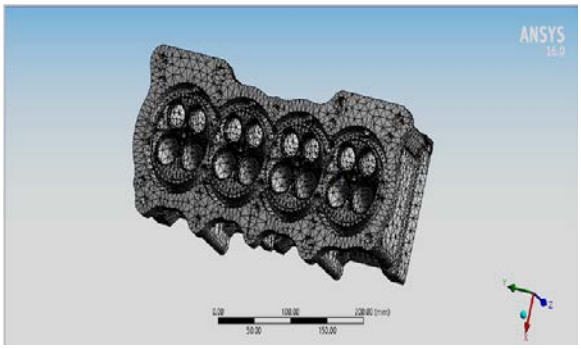

Figure.1.Cylinder head block

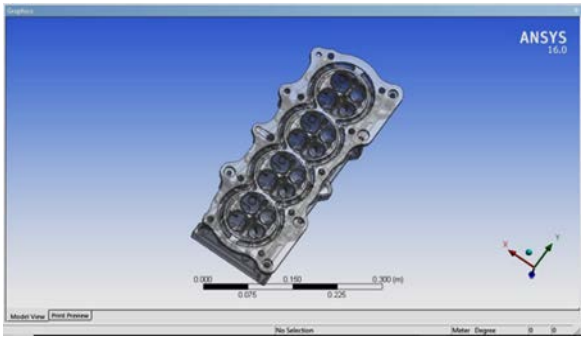

Figure 2: Mesh geometry of cylinder head

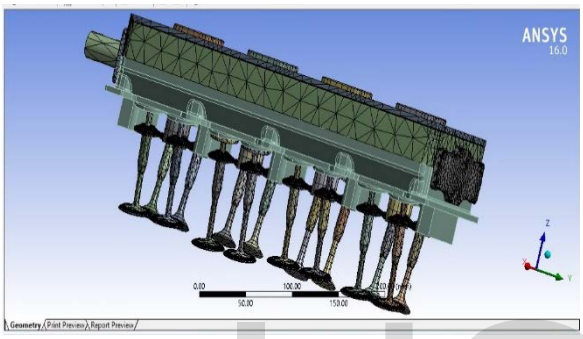

Figure 2a: Mesh geometry of head and valves

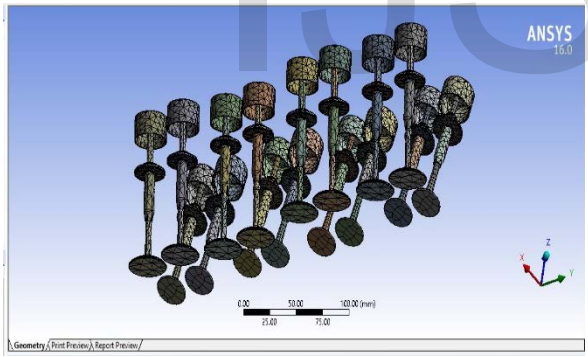

Figure 2b: Mesh geometry of inlet and exhaust valves

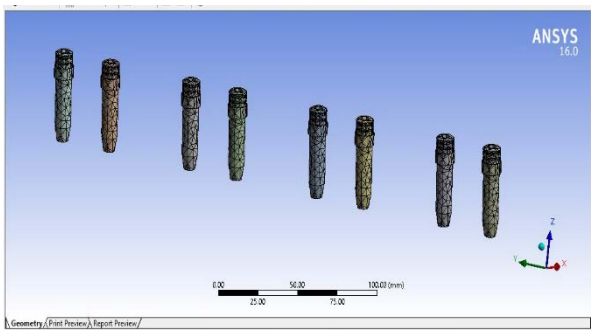

Figure 2c: Mesh geometry of valve guides

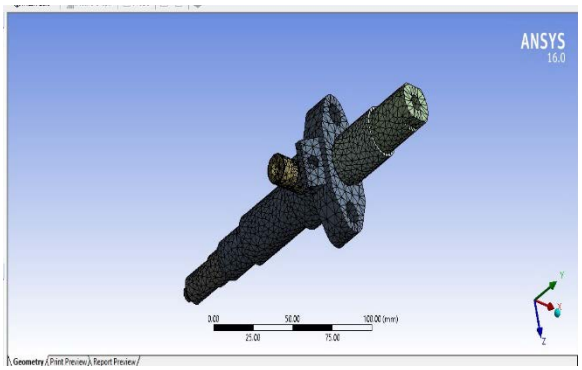

Figure 2d: Mesh geometry fuel injector

The cylinder head block (see Fig. 1) is formed of forged iron. It contains 2 intake valves (Fig. 1) and 2 exhaust valves (Fig. 1) product of cast steel. The valve guides, also because the valve seats, are pressed into the head. The exhaust-valve seats are cooled by cooling water flowing through the ring-shaped cavities around the seats. The fuel injector is set within the axis of the cylinder. the underside face of the plate, directly exposed to the in-cylinder gases, is cooled by special bores, which, however, represent an additional complication within the design of this automatically extremely loaded region of the plate.

3. THE FINITE ELEMENT ANALYSIS MODEL

The FEA model includes all parts mentioned in Table one. the important design of the cylinder head was slightly changed in details to modify manageable meshing. The model of the cylinder head block was created using the CAD model, in contrast to the models of different parts (valves, seats, valve guides and fuel-injector), that was developed directly in ABAQUS and CAE. Some elements of the valves and fuel-injector were significantly simplified or fully unseen, as they were thought of to possess a negligible influence on the results. a lot of info on the mesh geometry and statistics are provided in Fig. 2a and Table one.

3.1. Interactions and boundary conditions

Although the thermal loadings of engine elements vary significantly in time because of the alternate nature of engine operation, the computations were performed forward steady-state heat fluxes evaluated on the idea of time-averaged values. Taking into consideration the speed of the periodical changes and therefore the thermal inertia of the parts of the plate, the temperature variations are damped out inside a little distance from

the wall surface (~1mm), and this simplification is thus acceptable. The thermal contact interactions between individual elements of the plate assembly are represented by heat flux qAB from the solid face A to B, that is said to the distinction of their surface temperatures T_A, T_B consistent with

$$q_{AB} = K\,(T_B - T_A) \ldots\ldots\ldots (1)$$

where

K is the contact heat-transfer coefficient.

The boundary conditions of surfaces contacted by flowing gases are delineated as a steady-flow convective heat-transfer drawback, wherever the heat flux Q transferred from a solid surface at temperature T to a fluid at bulk temperature T_0 is decided from the relation,

$$q = h\,(T - T_0) \ldots\ldots\ldots (2)$$

Where h denotes the heat-transfer constant. this relies on the flow, the properties of the fluid and also the geometry of the surfaces. Useful varieties of these relationships are developed with the help of dimensional analysis. Within the case, the values of gas-side heat-transfer coefficients and bulk gas temperatures (i.e., for in-cylinder surfaces and intake and exhaust port walls) were obtained from an in-depth natural philosophy analysis of the engine in operation cycle performed with the employment of the 0-D thermodynamic model. This analysis uses the well-known empirical heat-transfer constant correlation.

Table1: Mesh statics of individual parts (Number of Nodes and Elements)

Part name	Nodes	Elements
Cylinder head	308018	182179
Inlet valve seat (2x)	157208	84776
Exhaust valve seat (2x)	139560	68496
Inlet valve seat (2x)	157208	84776
Exhaust valve seat (2x)	139560	68496
Inlet valve seat (2x)	157208	84776
Inlet valve guide	27256	14720
Exhaust Valve Guide	27256	14720
Fuel injector	35754	18781

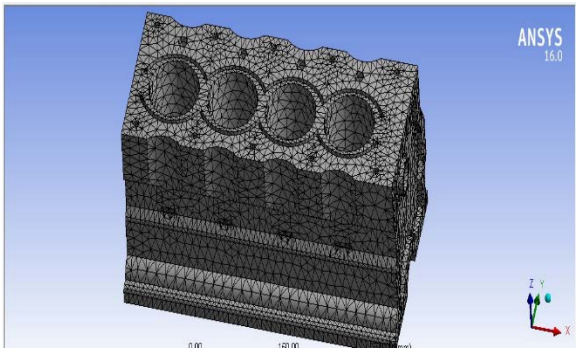

Figure 3: Geometry and Boundary conditions of a cylinder-head block

The remaining boundary conditions on outside surfaces most exposed to the ambient air temperature are described using estimated values of the heat transfer coefficient; In special cases, the heat-transfer is neglected. More detailed information on the used values is provided in Table 3 in conjunction with Fig. 3 and 4.

The coolant-side boundary conditions for the cool passages are supported values reportable within the literature. However, if native boiling happens at the surface, completely different relationships for h should be used. Heat-transfer coefficients for boiling options even additional difficult dependencies, since additionally to all or any the mentioned influences poignant the values of heat-transfer in convection, in boiling processes further variables play a job, e.g., those connected to the phase transition, microstructure, and material of the surface. Within the initial computed case (A) the chance of prevalence of native boiling effects was neglected. However, the computed results recommend that the boiling purpose of water was exceeded in some components of the cooling passages.

4. FINITE ELEMENT ANALYSIS

The method is predicated on the subdivision of the structures into parts with geometrically outlined characteristics.

Characters of the advanced structure are then resolved with the help of using algebra. The input file accommodates loading conditions on divided structures or meshes constraints with the physical properties of the fabric. Thermal loading involves the initial calculations of temperatures using boundary conditions on the gas facet, agent facet, and air facet

of the piston cylinder. The analysis bestowed during this paper is split into 2 sections, the temperature field distribution, and also the thermal stresses. The finite element technique with triangular element is employed to cut back the undulation formulation to a group of geometry equations. The expressions to calculate nodal temperatures and also the corresponding thermal stresses at each component are derived. the development of a finite element approach starts from the variational statement of the matter and using correct form perform a variety of geometry equations are developed that are capable the number of nodal parts within the problem domain. Then by minimizing the approximate perform a group of governing equation is developed for the piston and cylinder assembly.

These equations are solved by using a computer. A computer algorithm is developed to solve these equations in order to find the unknown parameters, that is, the temperature at different nodal points of the piston. A computer program is based on heat transfer through conduction, convection, matrix multiplication, matrix inversion, heat flow, and stiffness. By using these subroutine and main program, temperatures and heat flow field were calculated. Mathematical modeling of conduction equation, convection equation, and contact heat transfer equation has been done which is shown below.

The generalized governing differential equation for heat conduction can be represented as [14, 15]

$$K\nabla^2 T + q_E - \rho C\frac{\partial T}{\partial t} = 0 \ldots\ldots\ldots\ldots\ldots (3)$$

Where K is thermal conductivity in the radial (r) and axial (z) direction, respectively. qE is heat conduction per unit volume.ρ is the density of the material. C is the heat capacity of the material. T is temperature. t is time. The variational formulation for conductive boundary can be represented as [14, 15]

$$\frac{\partial x_k}{\partial\{t\}^e} = \begin{bmatrix} k_{11} & k_{12} & k_{13} \\ k_{21} & k_{22} & k_{23} \\ k_{31} & k_{32} & k_{33} \end{bmatrix} \begin{Bmatrix} t_i \\ t_j \\ t_k \end{Bmatrix} = [k]^{(e)}\{t\}^{(e)} \ldots\ldots\ldots\ldots (4)$$

where $[k]^{(e)}$ = stiffness matrix.

The generalized governing differential equation for contact boundary can be represented as [14, 15]

$$q_c = h_c(T^e - T^p) \ldots\ldots\ldots (5)$$

The variational formulation for contact boundary between 2elements (e) and (p) can be written as

$$X_{bcont} = \frac{h_c}{2}\int_{s_i}^{s_j}[\{t\}^{(e)} - \{t\}^{(p)}]2\pi r ds \ldots\ldots\ldots\ldots (6)$$

On solving it further in a similar fashion as done in convective boundary, it has been found that contact boundary variational integral of heat transfer after differentiation with respect to temperature of contact surface yields a set of linear equations as a contribution to the global set of equation.

Consider

$$\frac{(X_{bcont})_e}{\partial\{t\}^e} = \frac{2\pi h_c r_m r_{ij}}{6\cos\theta}\begin{bmatrix} 2-\frac{\varepsilon}{2} & 1 \\ 1 & 2+\frac{\varepsilon}{2} \end{bmatrix}\cdot\begin{Bmatrix} \{\{t_s\}^{(e)} - & \{t_s\}^{(p)}\}_1 \\ \{\{t_s\}^{(e)} - & \{t_s\}^{(p)}\}_2 \end{Bmatrix}\ldots\ldots\ldots (7)$$

The generalized governing differential equation for heat convection can be represented as [14, 15]

$$-K\left(\frac{\partial T}{\partial n}\right) = h(T - T_\infty) \ldots\ldots\ldots\ldots (8)$$

The variational formulation for convective boundary can be represented as

$$\partial_{X_{bconv}} = \int_A -K\left(\frac{\partial T}{\partial n}\right)\partial T\, dS = \int_A h(T - T_\infty)\,\partial T\, dS,$$

$$\frac{\partial(X_{bconv})_e}{\partial\{t\}^e} = \frac{2\pi h r_m r_{ij}}{6\cos\theta}\begin{bmatrix} 2-\frac{\varepsilon}{2} & 1 \\ 1 & 2+\frac{\varepsilon}{2} \end{bmatrix}\cdot\begin{Bmatrix} t_{si} \\ t_{sj} \end{Bmatrix} - \begin{Bmatrix} (ht_\infty)_1 \\ (ht_\infty)_2 \end{Bmatrix}\ldots\ldots\ldots\ldots\ldots (9)$$

where

$$r_m = \frac{r_i + r_j}{2}, \quad r_{ij} = r_j - r_i, \quad r_j = \frac{r_{ij}}{2}, \varepsilon = \frac{r_{ij}}{r_m} \ldots\ldots (10)$$

$$\frac{\partial(X_{bconv})_e}{\partial\{t_s\}} = [H]_s\{t\}_s - \{ht_\infty\} \ldots\ldots\ldots (11)$$

From (3), (5), and (11) variational integral of heat transfer globally is developed and represented as follow

$$\frac{\partial\{X\}^g}{\partial\{t\}^g} = \sum_{e=1}^{N}[k]^e\{t\}^e + [H]^e\{t\}^e - \{ht_\infty\}^e = 0 \ldots\ldots (12)$$

This equation can be written in its popular form as

$$([K] + [H])\{T\} = \{h_f\} \ldots\ldots\ldots\ldots (13)$$

Here $[K]$ is conduction matrix, $[H]$ is convection matrix, $\{T\}$is unknown temperature column vector at all nodal points, and $\{h_f\}$ is a column vector of known quantity. All above matrixes are global matrix of size $(N \times N)$, where N is the number of nodes. The column vector $\{h_f\}$ is of size $(N \times 1)$.

From (13), temperatures at all the nodes of the cylinder head are to be found out, which is to be represented in Figures 7–10.

After prediction of the temperature at all the nodes of the piston, radial thermal stress will be analyzed with the help of (14), (15), and (16) to show the radial strain, angular strain, and axial strain, respectively, as follows:

$$\varepsilon_r = \frac{\sigma_2}{E} - \frac{v}{E}\sigma_\theta - \frac{v}{E}\sigma_z + \alpha_t(T-T_0) \text{..... (14)}$$

$$\varepsilon_\theta = -v\frac{\sigma_r}{E} + \frac{1}{E}\sigma_\theta - \frac{v}{E}\sigma_z + \alpha_t(T-T_0) \text{..... (15)}$$

$$\varepsilon_z = -v\frac{\sigma_r}{E} - \frac{v}{E}\sigma_\theta - \frac{1}{E}\sigma_z + \alpha_t(T-T_0) \text{..... (16)}$$

Thus stress-strain relationship can be represented in matrix form as shown in equation

$$\begin{bmatrix} 1 & -v & -v \\ -v & 1 & -v \\ -v & -v & 1 \end{bmatrix} \begin{Bmatrix} \sigma_r \\ \sigma_\theta \\ \sigma_z \end{Bmatrix} = E\left[\begin{Bmatrix} \varepsilon_r \\ \varepsilon_\theta \\ \varepsilon_z \end{Bmatrix}\right] - \alpha_t(T-T_0) \begin{Bmatrix} 1 \\ 1 \\ 1 \end{Bmatrix} \text{..... (17)}$$

$$[P]\{\sigma\} = E[\{\varepsilon\}] \text{..... (18)}$$

Where

$[P]$ is the position matrix, σ_r = radial stress, σ_θ =angular stress, and σ_z = axial stress. After inversion of the position matrix, put the value of this in the above equation and find the stresses at all the nodes of the piston.

Consider

$$\{\sigma\} = [P]^{-1}E[\{\varepsilon\} - \{\varepsilon_o\}] \text{..... (19)}$$

$$[P]^{-1} = \frac{(1+v)(1-v)}{(1+v)^2(1+v)}\begin{bmatrix} 1 & v_1 & v_1 \\ v_1 & 1 & v_1 \\ v_1 & v_1 & 1 \end{bmatrix} \text{..... (20)}$$

$$\sigma = \frac{E(1-v)}{(1-2v)(1+v)}\begin{bmatrix} 1 & v_1 & v_1 \\ -v & 1 & v_1 \\ v_1 & v_1 & 1 \end{bmatrix}[\{\varepsilon\} - \{\varepsilon_0\}] \text{..... (21)}$$

Where σ = thermal stress, thermal strain $\{\varepsilon 0\} = (T - T0)$, and simple strain $\{\varepsilon\} = \begin{Bmatrix} \varepsilon_r \\ \varepsilon_\theta \\ \varepsilon_z \end{Bmatrix}$; V is the Poisson ratio and it is 0.33 and V1= $\frac{V}{1-V}$.

From (14), (16), and (21), radial displacement, axial displacement, and radial thermal stresses at all the nodes of the piston in cylinder head have been calculated and are represented in Figures4–7.

4.1. Finite Element Formulation for Checking Heat Balance.

This formulation can be used to check the heat balance of the problem. The amount of heat balanced is checked for accuracy and satisfied with the result by observing that the amount of heat supplied at gas side of the piston is equal to the amount of heat loss to both water and air side of the piston inside the cylinder head. Consider one side of an element having two nodal points i, which faced the boundary where heat is either supplied or rejected. The formulation of the equation is as follows.

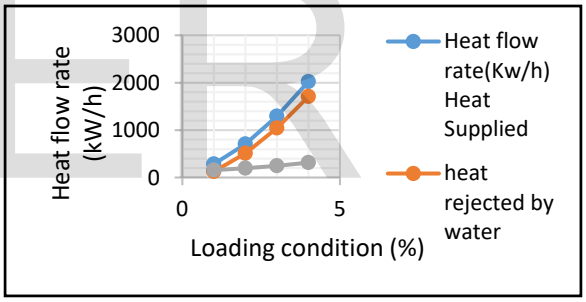

Figure 4: Heat flow pattern for four different load cases

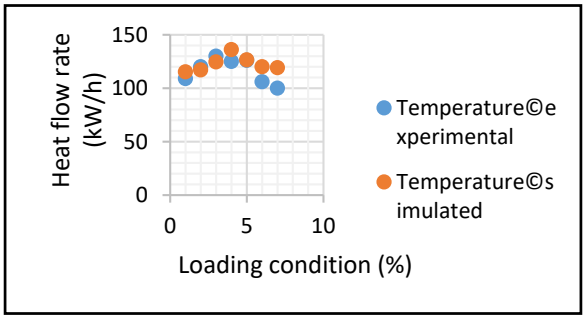

Figure 5: Temperature distribution at full load.

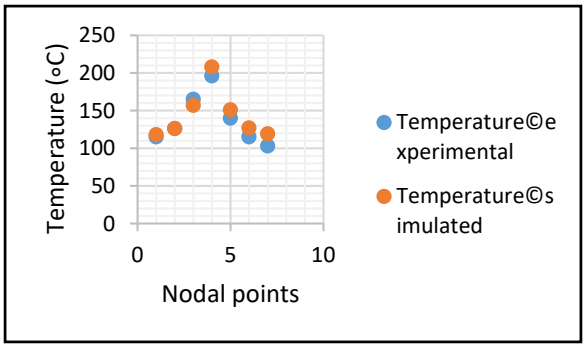

Figure 6: Temperature distribution at three-quarters load.

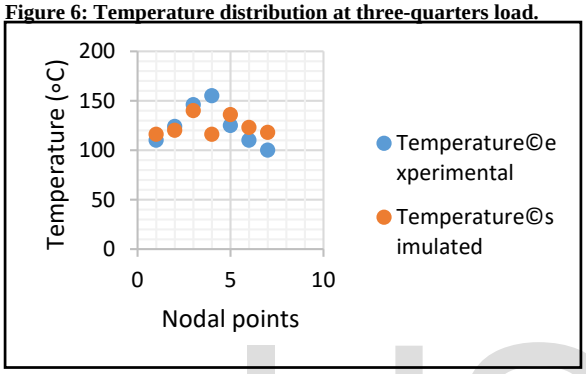

Figure 7: Temperature distribution at half load.

The generalized heat transfer equation from connective surfaces is represented as follows:

$$\int_{si}^{sj} dQ = \int_{si}^{sj} 2\pi rh(t_s - t_\infty)dS \ldots\ldots (22)$$

Where

$$t_s = C_1 + C_2S = [N_s]^{(e)}\{t_s\}^{(e)} \ldots\ldots\ldots (23)$$

$$\int_{r_i}^{r_j} dQ = \frac{2\pi h}{\cos\theta}\int_{r_i}^{r_j}\left(rN_{si}t_{si} + N_{sj}T_{sj} - T_\infty\right)dr \ldots (24)$$

Where

$$\int_{r_i}^{r_j} rN_{si}dr = \frac{r_{ij}r_m}{2}\left[1 - \frac{\varepsilon}{6}\right],$$

$$\int_{r_i}^{r_j} rN_{sj}dr = \frac{r_{ij}r_m}{2}\left[1 + \frac{\varepsilon}{6}\right],$$

$$\int_{r_i}^{r_j} rN_\infty dr = r_{rj}r_m t_\infty \ldots\ldots\ldots (25)$$

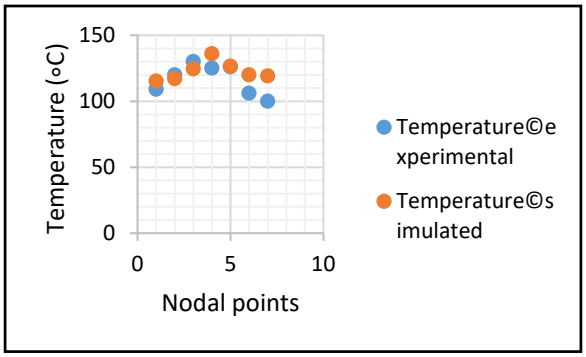

Figure 8: Temperature distribution at no load.

From (24), the heat transfer equation is developed and represented as follows:

$$Q_{sij} = \frac{2\pi h}{\cos\theta}\left[t_{si}\left(1 - \frac{\varepsilon}{6}\right)\frac{r_{ij}r_m}{2} + t_{sj} + \left(1 + \frac{\varepsilon}{6}\right)\frac{r_m r_{ij}}{2} - r_m r_{ij} t_\infty\right],$$

$$Q_{sij} = \frac{2\pi h r_m r_{ij}}{\cos\theta}\left[\left(1 - \frac{\varepsilon}{6}\right)\frac{t_{si}}{2} + \left(1 + \frac{\varepsilon}{6}\right)\frac{t_{si}}{2} - t_\infty\right]$$

$$r_m = \frac{r_i + r_m}{2}, \quad r_{ij} = r_j - r_i, \quad r_j = r_m - \frac{r_{ij}}{2}, \quad \varepsilon = \frac{r_{ij}}{r_m}$$

……. (26)

By using (26), heat transfer through different surfaces can be determined easily. Heat transfer from piston through combustion chamber side, airside, and waterside is represented by Q_g, Q_a, and Q_w, respectively.

5. DEVELOPMENT OF A GEOMETRICAL AND FINITE ELEMENT MODEL

A geometrical model of the engine cylinder head was developed based on the geometry of the actual object. Properties of the geometrical objects allowed determinant such parameters because of the cylinder diameter, the diameter of the piston pin hole, and dimensions of the piston ring grooves.

A final CATIA model is given in Figure one. during this model, a particular geometric simplification was assumed, as well as lost bends with a small radius on the sting of the crown and lateral surface of the head of the cylinder. Finally, the geometrical model was discretized into tetrahedron finite parts. Such parts had to be applied because of a complicated form of the cylinder internal surface. the size of finite parts was totally different in various sections of the cylinder; larger elements were used for the piston crown and

skirt, whereas the smaller ones were used near the oil channels. The full variety of nodes and parts within the quarter portion of cylinder internal surface Finite Element model was up to 311 and 272, severally. Figure two to figure 2d shows the fe distinct model of the cylinder block.

Table 2: Heat transfer parameter for four different cases of engine loading.

Parameter	Case 1 (No load)	Case 2 (1/2 load)	Case 3 (3/4 load)	Case 4 (Full load)
T_g combustion side) °n	405	605	805	1005
H_g(combustion side) w/m^{2}k	116.2	174.3	232.4	290.5

Table 3: Simulated and experimental temperature.

Parameter	No load	1/2 load	3/4 load	Full load
Heat Supply from combustion gases (Q_g) kw/hr	286	708	1239	2023
Heat rejection by water(Q_w) kw/hr	128	511	1043	1708
Heat rejection by air (Q_a) kw/hr	158	196	249	314

5.1. Thermal Boundary Conditions

The thermal boundary conditions accommodate applying for a convection heat transfer constant and therefore the bulk temperature, and that they are applied to the piston crown, seal landsides, seal groove lands, and cylinder internal surfaces. The temperature and warmth transfer coefficients within the combustion chamber all told the loading condition were known supported knowledge provided in a very previous analysis paper[14] that are given in Table 2. The adopted heat transfer constant on the contact surfaces are Ha (heat transfer coefficient at piston under crown surface) = 184.3 w/m2k, $H1$(heat transfer constant at ring lands and piston skirt higher and lower side) = 2805.4w/m2k, $H2$ (heat transfer constant at ring lands and piston skirt contact surfaces) = 22 w/m2k, $H3$ (heat transfer constant between piston rings and cylinder wall contact surfaces) = 39446 w/m2k, $H4$ (heat transfer constant between piston and cylinder wall contact surfaces)= 2114w/m2k, Hw (heat transfer constant through cylinder wall to water) = 1849.2w/m^{2}k and temperature on water aspect(Tw) was 125∘C and on housing side (Ta) was 85∘C.

6. RESULTS

The Heat flux distribution at flow field was studied with the assistance of finite part analysis exploitation thermal boundary conditions. to test the validity of the heat transfer model, the heat balance approached was adopted. The principle of conversion of energy, at steady state condition, the heat getting in the piston from the gas aspect is adequate the heat rejected to water and heat rejected to air. Figure 9 shows the variation of heat received (Q_g) by the piston from the recent gases, heat rejected to water (Q_w), and heat loss to air (Q_a) at the four totally different thermal loading conditions. It looks that heat received from the recent gas is inflated with an increase within the engine combustion temperature (Tg). Similarly, heat rejected to water and heat rejected to air increase with engine combustion temperature. Here within the gift analysis, the heat balance equation is happy for all the various loading conditions that, it will be determined that the error is incredibly little between heat equipped (Qg) by the combustion gasses and heat rejected to water (Qw) and air sides (Qa). It represents a standardized share throughout all the tests, shown in Table three. for sure, for steady state conditions the heat transfer rate will increase with engine loading condition, with a most determined at full load.

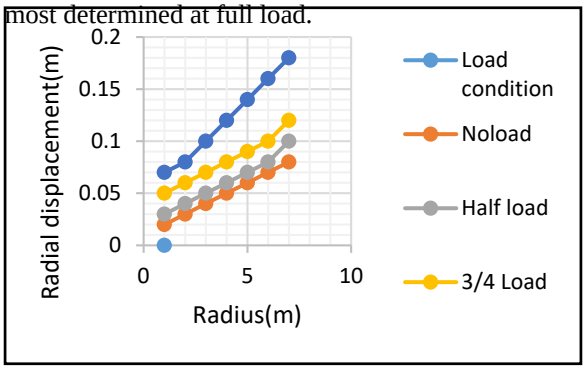

Figure 9: Radial displacement in section 1.

Figures 10–12 shows the temperature distribution. Through the analysis found that the utmost temperature occurs at the crown of the piston as a result of it's exposed to the hot gases within the combustion chamber, whereas the minimum temperature occurs at the carter end of the cylinder, that is exposed to the air. These variations in temperature are in the main liable for the development of temperature stress, causing the appearance of a

crack within the body of the piston in the cylinder head. Experimental setup established and scaled the temperatures through temperature sensors at different points (nodal points) wherever temperature sensors were mounted, shown in Table 4. Of course, for all load conditions, the simulated and experimental measured temperature raised with engine loading condition, with a maximum observed at full load.

Table 4: Simulated and experimental temperature.

Nodal points	Simulated Temperature (^{0}c)				Experimental Temperature (^{0}c)			
	No load	Half load	¾ load	Full load	No load	Half load	¾ load	Full load
1	115.1	116	118.9	121.6	109	110	115	122
2	117	120	126.2	132.9	120	124	126	130
3	124.4	139.1	157.8	182.0	130	146	165	195
4	135.3	116.1	208.6	261.0	125	155	196	250
5	125.6	136.1	151.1	169.1	125	125	140	158
6	119.8	123.1	127.5	133.1	105	110	115	120
7	118.0	118.8	119.9	121.2	100	100	103	108

The non-uniform variation in temperature is solely responsible for the development of thermal strain on piston body.

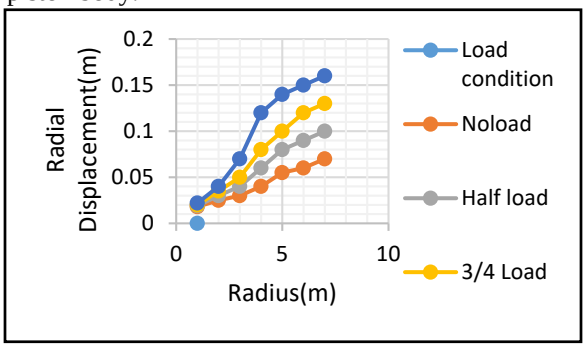

Figure 10: Radial displacement in section 2.

Initially, the piston is at 25°C and it's assumed that originally there's no thermal strain and stresses are present. Here within the analysis primarily, the displacement for every element is obtained and the compatibility equation is found to be satisfied. Being CST the strain within the whole element is constant and assumed to be set at the center of gravity of the element. So apart either expands or contracts to its temperature variation to keep up the constant strain within the whole element. The thermal strains are associated with stresses by suggests that of Hook's law of linear equal elastically. therefore the thermal stress developed depends directly on the mean temperature. this analyses on two different sections on the cylinder body are chosen to review the behavior of the strain. One section on the cylinder body is chosen close to the piston crown (section 1) having seven nodes and therefore the alternative inside of the body (section 2) having 7 nodes. Figures 11 and twelve show the radial displacements of the nodal points with regard to the piston radius below four thermal loadings at section1 and section 2, respectively. it had been found that the radial displacements of the nodes of those sections are varied in increasing order from the middle to the circumference of the piston altogether four loading conditions.

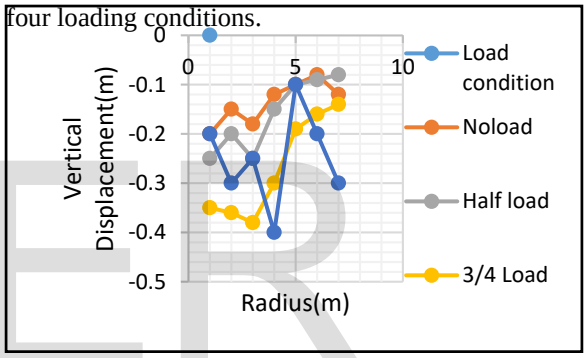

Figure 11: Vertical displacement in section 1.

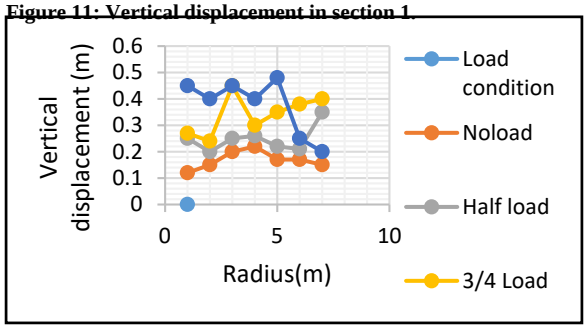

Figure 12: Vertical displacement in section 2.

And it's determined that the displacement of section 1 is quite that of section a pair of because of high temperature.

Figures 11 and 12 shows the vertical displacement of the nodal points with reference to the piston radius below four thermal loadings at sections 1 and2, respectively. Figures 11 and 12 indicate a sharp

variation in magnitude and direction of vertical displacement of nodal components. this can be as a result of each part tends to take care of constant strain property. If a node expands fora certain part then it should compress for one more element.

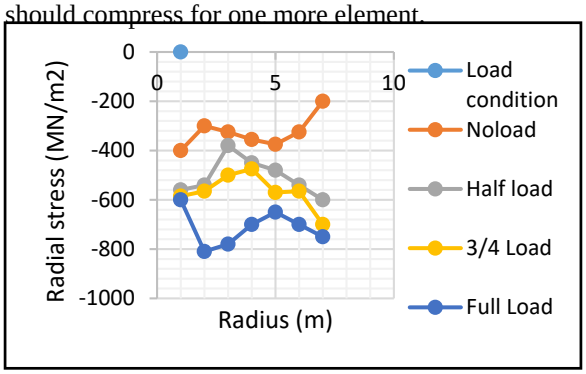

Figure 13: Variation in radial stresses in section 1.

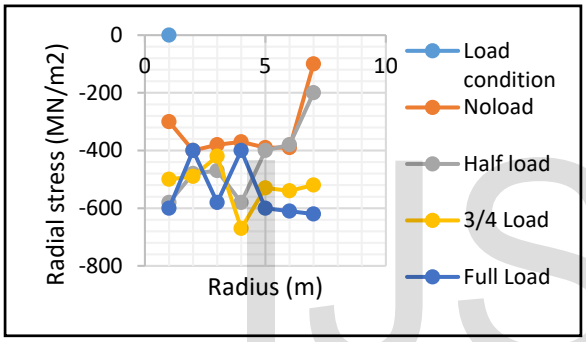

Figure 14: Variation in radial stresses in section 2.

Figures 13 and 14 shows the variation of radial stresses with respect to the piston radius under four thermal loadings at sections 1 and 2, respectively. These stresses are introduced in the body due to high temperature. Figures 13 and 14 show a sharp variation in magnitude and direction of radial stress.

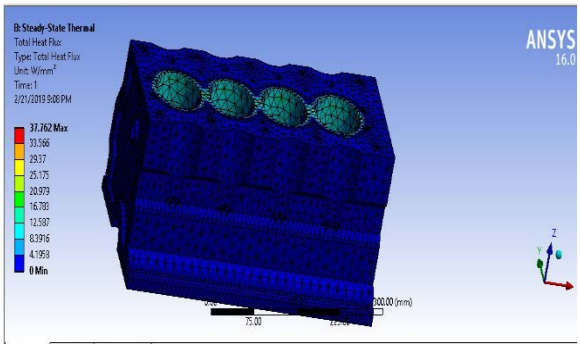

Figure15. Heat flux distribution by ANSYS

As discussed it is because every element tends to maintain the constant strain property. Thus it undergoes a simultaneous expansion or compression between two adjacent elements. However, by considering a very large number of elements these sharp variations in stress can be eliminated and more continuous curve can be obtained.

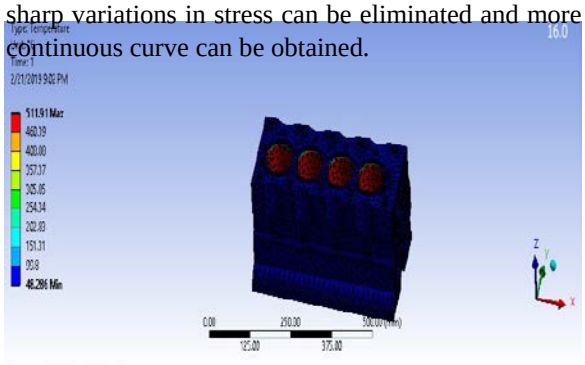

Figure16. Steady state thermal analysis by ANSYS

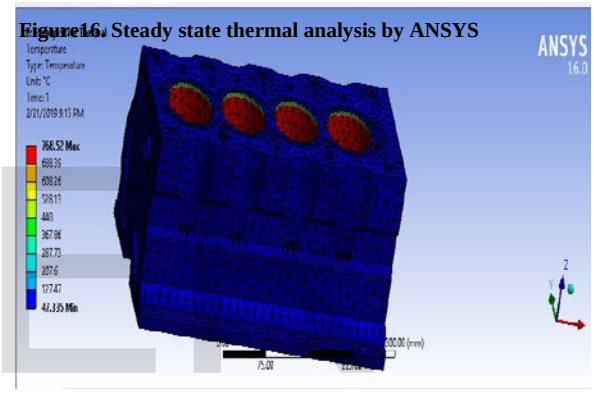

Figure17. Temperature distribution by ANSYS

7. CONCLUSIONS

As engine load will increase, the temperature of the piston and cylinder wall will increase exponentially and includes a positive relationship. The projected methodology may also be extended to see temperatures of different elements of the combustion chamber, after all taking under consideration its particularities. These temperatures, along with experimental measurements and therefore the estimations calculated, can be used to acquire associate integral heat engine losses model for the engine under analysis.

REFERENCES

[1]. Annand WJD (1986) "Heat transfer in the cylinder and porting. The thermodynamics and gas dynamics of

internal combustion engines", vol II. Oxford University Press, London

[2]. Woschni G (1967) "A universally applicable equation for the instantaneous heat transfer coefficient in the internal combustion engine". SAE Paper 670931

[3]. Han SB, Chung YJ, Kown YJ, Lee S (1997) "Empirical formula for instantaneous heat transfer coefficient in a spark ignition engine". SAE Paper 972995:219–226

[4]. Mohammadi A, Yaghoubi M, Rashidi M (2008) "Analysis of local convective heat transfer in a spark ignition engine". Int Commun Heat Mass Transf 33:215–224

[5]. Mohammadi A, Yaghoubi M (2010) "Estimation of instantaneous local heat transfer coefficient in spark ignition engines". Int J Therm Sci 49:1309–1317

[6]. Finol CA, Robinson K (2006) "Thermal profile of a modern passenger car diesel engine". SAE Paper 2006-01-3409

[7]. Cipollone R (1990) "on the thermal fields of I.C.E. cylinder liners". SAE Paper 900455

[8]. Norris PM, Wepfer W, Hoag KL, White KC (1993) "Experimental and analytical studies of cylinder head cooling". SAE Paper 931122

[9]. Jackson P, Addis B, Jun G, Tao SG, Sawant U (2008) "Development of a new 13L heavy-duty diesel engine using analysis—led design". SAE Paper 2008-01-1515

[10]. Etemad S, Wallesten J, Stein CF, Eriksson S, and Johansson K (2005) "CFD-analysis of cycle averaged heat flux and engine cooling in an IC-engine". SAE Paper 2005-01-0200

[11]. Koch F, Decker P, Gulpen R, Quadflieg J, Leoprecht M (1998) "Cylinder liner deformation analysis—measurements and calculations". SAE Paper 980567

[12]. Londhe A, Yadav V, Mulemane A (2009) "A multidisciplinary approach for evaluating the strength of engine cylinder head and crankcase assembly under thermos structural loads". SAE Paper 2009-01-0819

[13]. Etemad S, Hagner T (2007) "Accurate modeling of the thermal behavior of a diesel engine by means of CFD and its validation". SAE Paper 2007-01-1905

[14]. J. Chang, O. Guralp, Z. Filipi et al., "New heat transfer correlation for an HCCI engine derived from measurements of instantaneous surface heat flux," SAE 2004-01-2996, 2004.

[1]5. S. K. Sharma, P. K. Saini, and N. K. Samaria, "Modelling and analysis of radial thermal stresses and temperature field in diesel engine valves with and without air cavity," *International Journal of Engineering, Science and Technology*, vol. 5, no. 3, pp. 111–123,2013.